Cavity ring-down spectroscopy and vibronic activity of benzo[ghi]perylene

Xiaofeng Tan[a] and Farid Salama
Space Science Division, National Aeronautics and Space Administration (NASA) Ames Research Center, Mail Stop 245-6, Moffett Field, California 94035-1000

(Received 4 March 2005; accepted 28 April 2005; published online 12 July 2005)

Gas-phase cavity ring-down spectroscopy of jet-cooled benzo[ghi]perylene ($C_{22}H_{12}$) in the 26 950–28 600-cm^{-1} spectral range is reported for the first time. This study is part of our extensive laboratory astrophysics program for the study of interstellar polycyclic aromatic hydrocarbons. The observed spectrum shows an intermediate level structure and significant broadening and is associated with the vibronically coupled $S_1(^1A_1) \leftarrow S_0(^1A_1)$ and $S_2(^1B_1) \leftarrow S_0(^1A_1)$ electronic transitions. Time-dependent density-functional calculations were performed to calculate the energetics, vibrational frequencies, and normal coordinates of the S_1 and S_2 states. A simple vibronic model was employed to account for the vibronic interaction between the vibronic levels of the S_1 and S_2 states. The calculated vibronic spectrum is found to be in good agreement with the experimental spectrum. © *2005 American Institute of Physics*. [DOI: 10.1063/1.1938907]

I. INTRODUCTION

There have been extensive experimental and theoretical studies on polycyclic aromatic hydrocarbons (PAHs). PAHs have been suggested to be the possible molecular carriers of the ubiquitous diffuse interstellar bands (DIBs) seen in absorption in the spectra of stars obscured by diffuse interstellar clouds.[1–6] The very low-vapor pressure of PAHs makes it extremely difficult to measure the absorption spectra of these species in the gas phase with conventional spectroscopic techniques. This is particularly true for middle and large size PAHs (≥20-C-atom molecules). Earlier experimental data were primarily obtained with matrix-isolation spectroscopy (MIS) due to its capability of accumulating PAHs in cryogenic inert-gas solid matrices over a period of time until the concentration reaches the detection threshold.[7–9] The spectral features recorded with MIS, however, are shifted and broadened due to the interaction of the trapped species with the solid lattice. In recent years, the cavity ring-down spectroscopy (CRDS),[10–13] a high sensitivity direct absorption technique, has gained an increasing popularity in this field of research. However, only a limited number of PAHs have been studied by CRDS to date,[14–20] mainly due to the difficulty of bringing these low-vapor pressure molecules into the gas phase in amounts detectable under the laboratory conditions that are relevant for astrophysical studies.

In a recent paper,[20] we presented the cavity ring-down spectroscopy and theoretical calculations of the $S_1 \leftarrow S_0$ transition of perylene ($C_{20}H_{12}$). The agreement between the calculation and the experiment is particularly good for this molecule. Perylene, however, probably represents an extreme case where spectroscopic perturbations are very small. In this extreme case, distinguishable vibrational progressions that mainly consist of totally symmetric modes are predominant in the observed spectra. The bandwidths of the spectral features are well determined by the rotational contour of the molecule and show small homogenous broadening. PAHs, and, in particular, PAH ions, on the other hand, are generally characterized by a large density of electronic states in small energy ranges due to their conjugated π electron systems. In these systems, limited separations among the electronic states lead to the breakdown of the Born–Oppenheimer (BO) approximation and result in strong perturbations such as vibronic and spin-orbit interactions. The spectra of these systems usually exhibit complex structures and are characterized by large homogeneous broadening. Conventional quantum-chemical methods built on the BO approximation are often found to be inadequate in predicting the spectra of these conjugated systems. It is worthy pointing out that the bandwidths of the DIBs vary significantly and range from 2 to130 cm^{-1}. If PAHs indeed represented a major family of the carriers of the DIBs, the distribution of the bandwidths of the DIBs would provide useful information on the nature of the PAH species that are responsible. For this purpose, more experimental and theoretical work on different PAH species are needed.

As an extension to our previous work on perylene,[20] we present in this paper a combined experimental and theoretical study of benzo[ghi]perylene ($C_{22}H_{12}$). To the best of our knowledge, the gas-phase absorption spectrum of this molecule has not been reported before. This paper is organized as follows: the description of the experimental setup and the CRDS spectrum of benzo[ghi]perylene are presented in Sec. II; the results of the time-dependent density-functional calculations and the calculations of the vibronic interaction are presented in Sec. III; the assignment of the spectra is also discussed in this section; and further discussions are presented in Sec. IV.

[a]Authors to whom correspondence should be addressed. Electronic mail: x.tan@jhu.edu; farid.salama@nasa.gov

II. EXPERIMENT

A. Apparatus

The experimental apparatus has been described in detail previously.[15,16,20] In brief, a pulsed supersonic beam containing benzo[ghi]perylene (Sigma-Aldrich, 98.8%) seeded in Ar was prepared with a pulsed discharge slit nozzle (PDN).[21] The PDN consists of a heated copper sample reservoir and a 10-cm-long by 200-μm-wide slit, which is sealed from inside by a Vespel (Dupont, SP-22 Grade) slit poppet driven by three synchronized pulsed solenoid valves (General Valve Series 9). Two stainless knife-edge electrodes are mounted outside the PDN on each side of the slit. The two electrodes are separated by an even gap of 400 μm and configured as the cathode of a high-voltage pulse generator. The PDN assembly itself is configured as the anode. This design enables the generation of atomic and molecular ions and radicals in the jet expansion. In the experiment, the high voltage was applied only for the wavelength calibration, which was achieved by monitoring the Ar^* atomic lines generated in the discharge. Benzo[ghi]perylene was placed on the bottom of the heated sample reservoir to ensure adequate evaporation.

The supersonic beam containing benzo[ghi]perylene and Ar was probed by cavity ring-down spectroscopy. The spectra were probed using frequency-doubled output of a Nd:yttrium aluminum garnet (YAG) (Quanta-Ray Lab 150 from Spectra-Physics) pumped dye laser (Quanta-Ray PDL-2 from Spectra-Physics). A mixture of three dyes of LDS 751, LDS 750, and LDS 698 (Exciton) were used. The bandwidths were 0.18 and 0.7 cm^{-1} for the fundamental and doubled output, respectively. The ring-down cavity consists of two high-reflectivity (99.9% at 365 nm) concave (6-m curvature radius) mirrors (Los Gatos Research) mounted 55 cm apart. The typical ring-down time was 5 μs. The ring-down signal was collected by a photosensor module (H6780-04 from Hamamatsu) and digitized by a 20-MHz 12-bit acquisition board (Adlink, PCI9812). The data were then processed by a personal computer (PC) program and the cavity losses were extracted.

B. Results

Figure1 presents a cavity ring-down spectrum of benzo[ghi]perylene in the 26 950–28 600-cm^{-1} (349.7–371.1 -nm) spectral range. The spectrum was recorded 2 mm downstream of the slit nozzle with the PDN assembly maintained at a stable temperature of 295 °C. The backing pressure of Ar was 1.0×10^5 Pa, and the background pressure was 10.5 Pa. A number of vibronic bands were observed in this spectral region. The bands are labeled alphabetically in the figures. We fitted the observed bands to Gaussian profiles. The fitted positions and Gaussian widths are listed in Table I. We could not observe these bands when the PDN assembly was kept at room temperature. The spectra became weak but remained essentially unchanged when Ne was used as the carrier gas. The observed strongest band *F* was found to be blueshifted by ~3 nm from the strongest band of benzo[ghi]perylene isolated in a Ne matrix.[22] We were advised by Sigma-Aldrich of the possible presence of trace perylene and coronene in benzo[ghi]perylene. A comparison with the gas-phase spectra of these two molecules is therefore recommended to eliminate a possible contribution from these two molecules to the observed spectrum. In the absence of gas-phase data of these two molecules in the spectral range of interest, we proceeded as follows. In the case of perylene, we ran a check experiment under the same experimental conditions. No spectral features were observed, definitely eliminating perylene as a contributor to the spectrum. In the case of coronene, we estimated its concentration to be ca. 10^{-4} of that of perylene under the experimental conditions.[23] Based on the temperature used in our previous experiment (217 °C) on perylene[20] and that used in this experiment

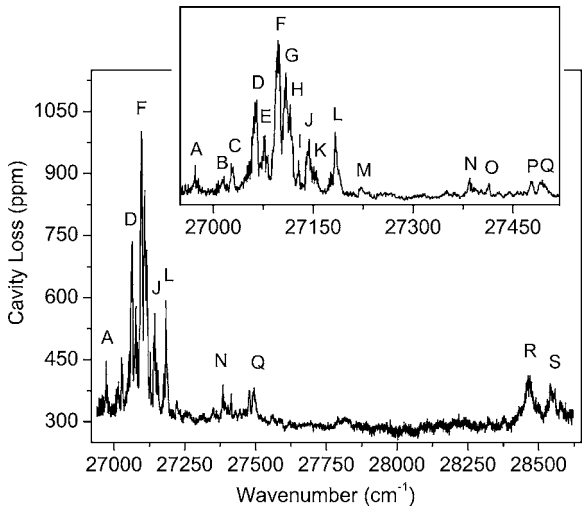

FIG. 1. Cavity ring-down spectrum of benzo[ghi]perylene in the 26 950–28 600-cm^{-1} spectral range. The inset panel shows the spectral features in the 26 950–27 520-cm^{-1} spectral range. Benzo[ghi]perylene was heated to 295 °C and prepared in a jet expansion with Ar buffer gas. The spectra were recorded 2 mm downstream of the PDN slit nozzle. The backing pressure was 1.0×10^5 Pa and the background pressure in the chamber was 10.5 Pa.

TABLE I. Band positions and Gaussian widths for bands in the cavity ring-down spectrum of jet-cooled benzo[ghi]perylene.

Band	Position[a]	Width[a]
A	26 972.5(6)	5.3(10)
B	27 014.4(6)	4.6(10)
C	27 028.3(6)	5.0(5)
D	27 062.8(6)	7.3(8)
E	27 076.5(6)	4.5(10)
F	27 096.8(6)	7.5(5)
G	27 108.0(6)	6.9(7)
H	27 116.3(8)	5.1(10)
I	27 127.6(6)	3.1(7)
J	27 142.9(6)	6.5(6)
K	27 153.3(6)	7.1(13)
L	27 184.1(6)	6.4(4)
M	27 222.3(6)	5.1(7)
N	27 384.9(6)	4.1(6)
O	27 413.6(6)	2.8(5)
P	27 477.8(6)	5.1(3)
Q	27 494.3(6)	12.5(8)
R	28 465.7(6)	26.7(10)
S	28 546.4(6)	24.7(38)

[a]The values are in units of cm^{-1}.

(295 °C) and the absorption intensities observed in these two experiments, we estimated the concentration of benzo[ghi]perylene to be ca. 10^{-2} of that of perylene under the experimental conditions. Trace coronene (<1%) in the sample can thus produce only a concentration of gas-phase coronene that is ca. 10^{-4} of that of benzo[ghi]perylene under the experimental conditions. As shown later in this paper, the oscillator strength of the observed transiton of benzo[ghi]perylene is 0.27, it is therefore not possible for trace coronene to contribute to the observed spectral features. Based on these observations, we unambiguously assign all the observed spectral features to benzo[ghi]perylene.

III. THEORY

A. Density-functional calculations

To interpret the observed spectrum, we have carried out density-functional theory[24–26] (DFT) and time-dependent density-functional theory[27,28] (TDDFT) calculations of the vertical transition energies, vibrational frequencies, and normal coordinates of several low-lying singlet and triplet electronic states of benzo[ghi]perylene. The vertical transition energies were calculated with the Becke's 3-parameter exchange functional[29] and the correlation functional of Lee, Yang, and Parr[30,31] (B3LYP). To reduce the computational cost, the vibrational frequencies and normal coordinates were calculated with the Becke (B88) (Ref. 32) exchange functional, the Perdew (P86) (Ref. 33) correlation functional (BP86), and the resolution of identity (RI) approximation.[34,35] The RI approximation allows for efficient computation of the electronic Coulomb interaction and leads to more than a tenfold speedup compared to the conventional method. In all calculations, the split valence polarization[36] (SVP) basis set ([3*s*2*p*1*d*]/[2*s*1*p*]) was used. The calculations of the excited states were performed within the Tamm–Dancoff approximation[37] (TDA) and the random phase approximation (RPA),[38,39] respectively. For all the DFT and TDDFT calculations the TURBOMOLE 5.7 code[40] was used. The geometries of the ground and excited states were optimized by using the analytical DFT and TDDFT gradients, respectively. The vibrational frequencies and normal coordinates of the ground and excited states were, respectively, calculated analytically and numerically. A scale factor of 0.99 is used for all the normal frequencies that were obtained from the BP86/SVP calculations. The coordinate system used in the calculations is shown in Fig. 2. The C_{2v} point group was used in the calculations.

B. Assignment of the spectrum

The vertical transition energies and oscillator strengths (length form) of the four lowest singlet excited states (S_1-S_4) and the six lowest triplet states (T_1-T_6) of benzo[ghi]perylene obtained from B3LYP/SVP with the TDA are listed in Table II. Excitation energies obtained with the RPA are also shown in Table II in the parentheses for comparison. Unless otherwise specified, theoretical excitation energies mentioned thereafter refer to those obtained from the TDA. In the calculation, the first excited singlet state (27 217 cm^{-1}) was predicted to be a $^1A_1$ state (^1L_b in the Platt nomenclature[41]) with an oscillator strength factor of 2.7×10^{-4} while the second excited singlet state (27 401 cm^{-1}) was predicted to be a $^1B_1$ state (^1L_a in the Platt nomenclature) with an oscillator strength factor of 0.27. The excitation energies of these two singlet states fall inside the scanned 26 950–28 600-cm^{-1} spectral range. The next excited singlet state is far high in energy and cannot contribute to the observed features. It is therefore reasonable to assign the observed spectra to the $S_2(^1B_1)\leftarrow S_0(^1A_1)$ electronic transition of benzo[ghi]perylene as the S_2 carries a much larger oscillator strength factor than the S_1 state. This assignment is consistent with the assignment of Nijegorodov *et al.* of the benzo[ghi]perylene spectra obtained in a cyclohexane solution.[42] At almost the same time, Chillier *et al.* published the spectra of benzo[ghi]perylene isolated in a Ne matrix.[22]

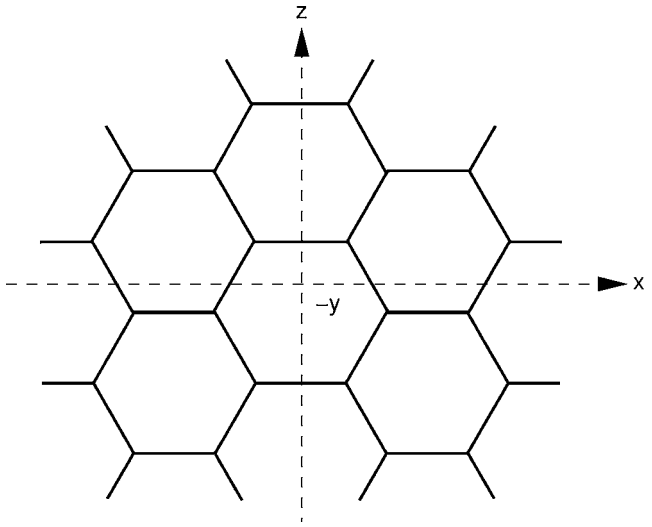

FIG. 2. The coordinate system used in the (TD)DFT calculations of benzo[ghi]perylene. The calculations were performed in the C_{2v} symmetry.

TABLE II. Excitation energies and oscillator strengths of benzo[ghi]perylene.

State	Excitation energy (cm^{-1}) B3LYP/SVP[a]	Excitation energy (cm^{-1}) Expt.	Oscillator strength[b]
$S_1(^1A_1)$	27 217 (27 113)	25 795[c], 25 787[d], 24 660[e]	0.000 27
$S_2(^1B_1)$	27 401 (26 123)	27 132[c], 26 992[f], 25 970[e]	0.27
$S_3(^1B_1)$	32 702 (32 584)		0.0013
$S_4(^1A_1)$	35 301 (33 569)	34 516[d], 34 411[f]	0.42
$T_1(^3B_1)$	18 177 (16 138)	17 227[d], 16 100[e]	
$T_2(^3A_1)$	24 726 (24 191)		
$T_3(^3A_1)$	26 305 (26 120)		
$T_4(^3B_1)$	28 063 (26 778)		
$T_5(^3B_1)$	28 889 (27 838)		
$T_6(^3A_1)$	29 036 (27 594)		

[a]Vertical transition energies calculated at the B3LYP/SVP level of theory with the TDA and RPA methods. Values calculated with the RPA are listed in the parentheses.
[b]Length form.
[c]This work.
[d]Estimated excitation energies in the gas phase by assuming same spacings between the spectral features in the gas phase and those in the solution (Ref. 42).
[e]From Ref. 42.
[f]From Ref. 22.

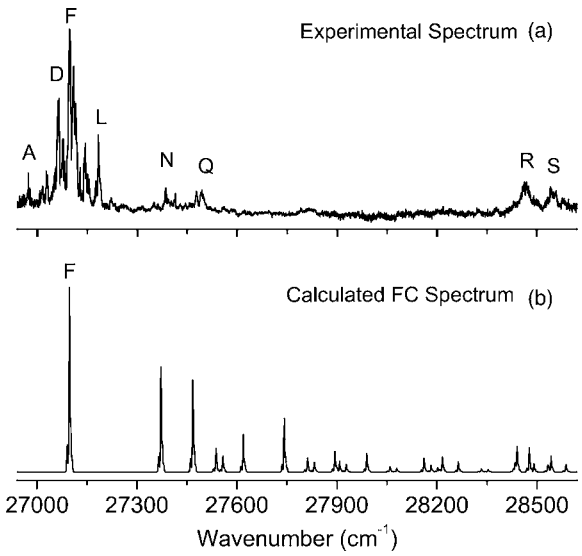

FIG. 3. Comparison of the (a) experimental and (b) calculated Franck–Condon spectra of the $S_2 \leftarrow S_0$ transition of benzo[ghi]perylene. The calculated spectrum is convoluted with a Gaussian function of $\sigma = 3.0\ \mathrm{cm}^{-1}$ and the bands are shifted so that the calculated 0-0 band falls at the same position as that of band *F*. The vibrational frequencies and normal coordinates are calculated at the BP86/SVP level of theory.

In this paper, however, the same transition was assigned to the $S_1 \leftarrow S_0$ electronic transition based on the TDDFT calculations. It has been shown by Parac and Grimme that, for large unsaturated π systems, TDDFT within the RPA in general underestimates the excitation energy of the ^1L_a state and overestimates the excitation energy of the ^1L_b state.[43] This often results in an inversion of the ordering of the excitation energies of the first two excited singlet states in these conjugated π systems. As shown in Table II, this argument applies to benzo[ghi]perylene. A close inspection of the MIS spectra of benzo[ghi]perylene in the Ne matrix (Fig. 1 of Ref. 22) shows that the signal at the expected position ($\sim$390 nm by assuming the same spacing from the strongest peak as observed in the cyclohexane solution) of the weak $S_1 \leftarrow S_0$ transition is very noisy. This weak transition was probably buried by the noise in the MIS spectra and not observed by these authors. We list in Table II the experimental excitation energies derived from this work and from previous MIS (Ref. 22) and solution[42] experiments. We also list in Table II the estimated gas-phase excitation energies by assuming same spacings between the spectral features in the Ne matrix and those in the cyclohexane solution. From Table II, we conclude that the TDA is superior to RPA in predicting the excitation energies of neutral benzo[ghi]perylene.

As shown in Table II, the S_2 state is close in energy to the S_1 state ($\sim$1310 cm^{-1} as determined in Ref. 42). The limited separation between the S_1 and S_2 states is smaller than the vibrational frequencies of many normal modes of the molecule. This results in strong vibronic interactions and the breakdown of the BO approximation. To show this point, we calculated the $S_2 \leftarrow S_0$ spectrum of benzo[ghi]perylene with the Franck–Condon approximation within the BO approximation. A comparison of the calculated Franck–Condon spectrum with the experimental spectrum is shown in Fig. 3. The Franck–Condon (FC) factors were evaluated using the MOLFC computer code developed by Borrelli and Peluso.[44] In the Franck–Condon calculations, only the totally symmetric modes are included with the exception of the two lowest normal modes. These two modes are of a_2 (60.5 cm^{-1} in S_0) and b_2 (92.1 cm^{-1} in S_0) symmetries and are included because they are expected to have significant excitation due to their low frequencies in the S_0 state. A vibrational temperature of 70 K is assumed for all modes in the calculation. The calculated spectrum is convoluted with a Gaussian function with $\sigma = 3.0\ \mathrm{cm}^{-1}$. The chosen vibrational temperature and Gaussian width are based on the results of our previous work on perylene[20] that was done under very similar experimental conditions.

It is clear from Fig. 3 that the agreement between the calculated spectrum and the experimental spectrum is poor. The agreement between the calculation and the experiment is particularly poor in the 26 950–27 300-cm^{-1} spectral range. In this spectral range, features associated with the 0-0 transition and few hot-band satellite transitions are seen in the calculated spectrum, which can only be roughly associated with the strongest band *F* (27 097.5 cm^{-1}) observed in the experimental spectrum. Bands *A*-*E* and *G*-*M*, however, are all missing in the calculated spectrum. We attribute these features to nearby background vibronic states in the S_1 ($^1A_1$) manifold that are magnified by the intensity borrowing effect through the strong vibronic interactions between the S_1 and S_2 states. The structure of the observed spectral features, which are caused by the strong vibronic interactions between the S_1 and S_2 states, is known as an intermediate level structure. The same type of structure has been reported for pyrene,[18,45,46] naphthalene,[47] azulene,[48] phenanthrene,[49] and quinoxaline.[50]

C. Vibronic model

To correctly reproduce the observed spectrum, the vibronic interaction between the S_1 and S_2 states should be properly taken into account in the calculations. In this section, we will introduce a simple vibronic model to account for the vibronic interaction between the S_1 and S_2 states of benzo[ghi]perylene. We closely follow in our model the approach used by Ohta *et al.*[45] Since the S_2 ($^1B_1$) state carries an oscillator strength that is ca. 10^3 times larger than that of the S_1 ($^1A_1$) state, we assume that the vibronic levels of S_1 of B_1 symmetry borrow intensities from vibronic levels of S_2 of B_1 symmetry. The resulting mixed states can be expressed as a linear combination of these vibronic levels as follows:

$$\Psi_n = a_2^n \Psi_2 + \sum_k b_k^n \Psi_1^k = a_2^n |\phi_2\rangle \prod_i |X_2^{m(i)}\rangle + \sum_k b_k^n |\phi_1\rangle \prod_i |X_{1k}^{g(i)}\rangle, \quad (1)$$

where Ψ_n is the mixed vibronic state, Ψ_2 is a discrete vibronic level belonging to S_2 of B_1 symmetry, and Ψ_1^k is a manifold of the vibronic levels of S_1 of B_1 symmetry. $|\phi_1\rangle$ and $|\phi_2\rangle$ are, respectively, the electronic wave functions for the S_1 and S_2 electronic states, while $|X_{1k}^{g(i)}\rangle$ and $|X_2^{m(i)}\rangle$ are, respectively, the vibrational wave functions of the S_1 and S_2

manifolds. The indices m and g represent the vibrational quantum number in the ith vibrational mode. The electronic wave functions and the vibrational wave functions are obtained from the TDDFT calculations within the BO approximation. The transition intensity of the mixed vibronic state Ψ_n is determined by $|a_2^n|^2$. In our model, the vibronic function Ψ_2 is assumed to consist of totally symmetric a_1 vibrational modes while the vibronic function Ψ_1^k is assumed to consist of a b_1 vibrational mode and f quanta of a_1 vibrational modes, i.e.,

$$\prod_i |X_{1k}^{g(i)}\rangle = |X_{1k}^{1(\mu)}\rangle \prod_{i\neq\mu} |X_{1k}^{p(i)}\rangle, \tag{2}$$

where μ represent the b_1 vibrational mode and $\Sigma_{i\neq\mu} p=f$. The interaction between the vibronic levels of the S_1 manifold is assumed to be negligible. The off-diagonal matrix elements are therefore expressed as follows:[45]

$$V' = \langle \phi_1 | \partial H/\partial Q_\mu | \phi_2 \rangle \langle X_{1k}^{1(\mu)} | Q_\mu | X_2^{0(\mu)} \rangle \cdot \prod_{i\neq\mu} \langle X_{1k}^{p(i)} | X_2^{m(i)} \rangle$$

$$\equiv V_{12}(Q_\mu) \cdot \prod_{i\neq\mu} \langle X_{1k}^{p(i)} | X_2^{m(i)} \rangle, \tag{3}$$

where $V_{12}(Q_\mu)$ is the vibronic coupling (VC) matrix element and $\Pi_i \langle X_{1k}^{p(i)} | X_2^{m(i)} \rangle$ is the Franck–Condon integral that can be easily extracted from the TDDFT calculations.

Ohno and co-worker,[51,52] have shown that conventional quantum-chemical methods fail to predict a reliable harmonic frequency for a strongly vibronically active mode. In such a case, dramatic frequency upshift (coupling with a lower vibronic state) or downshift (coupling with a higher vibronic state) and change of vibrational mode form can be observed for this mode. The frequency shift is usually a good measure of the strength of the vibronic activity of the corresponding mode. In our vibronic model, we consider that the vibronic coupling is the only source of the frequency shift. This amounts to the assumption that the frequencies of the b_1 mode of the S_1 state should asymptotically tend to the ground-state frequencies. We therefore rewrite Eq. (3) as follows:

$$V' = \lambda_\mu \cdot |\omega_\mu^0 - \omega_\mu^1| \cdot \prod_{i\neq\mu} \langle X_{1k}^{p(i)} | X_2^{m(i)} \rangle, \tag{4}$$

where ω_μ^0 and ω_μ^1 are the vibrational frequencies of the b_1 mode of the S_0 and S_1 electronic states that can be obtained from (TD)DFT calculations. λ_μ is a parameter to be determined. To estimate the value of λ_μ, we examine a two-level system in which the two interacting diabatic states have energies V_1 and V_2 and an off-diagonal element V_{12}. Without losing generality, let $V_1 > V_2$. We also assume a weak-interaction scenario in which $V_1 - V_2 \gg V_{12}$. It can readily be shown that the energies of the two adiabatic states to be $V_1 + V_{12}/2$ and $V_2 - V_{12}/2$. Therefore, as the first-order approximation, we set λ_μ to be 2. The final values of λ_μ can always be determined by fitting to the experimental data.

D. Results of the vibronic calculations

In the present case of benzo[ghi]perylene, we focus on the treatment of the vibronic features in the 26 950–27 300 -cm^{-1} spectral range that are associated with the $S_2(0)$ vibronic level. In the calculations, we set $f=3$ and the resonance range to be ±500 cm^{-1} of the energy of $S_2(0)$. All configurations that fall out of the resonance range were ignored in the calculations. The initial energy separation between $S_1(0)$ and $S_2(0)$ was set to 1310 cm^{-1} as determined in Ref. 42. There are 33 a_1 modes and 32 b_1 modes of benzo[ghi]perylene, but only 27 a_1 modes and 26 b_1 modes of S_1 can contribute to the vibronic configurations that fall inside the chosen resonance range.

TABLE III. Calculated frequencies of the 27 a_1 modes and 26 b_1 of S_1 that are used in the vibronic calculations, and values of $|\omega_\mu^0 - \omega_\mu^1|$.

b_1 mode	Frequency	$\lvert\omega_\mu^0-\omega_\mu^1\rvert$	a_1 mode	Frequency
$\underline{1}$	352.5	2.4	1	274.4
$\underline{2}$	392.0	8.5	2	370.6
$\underline{3}$	509.1	8.9	3	439.5
$\underline{4}$	533.2	21.3	4	460.0
$\underline{5}$	600.1	8.5	5	521.6
$\underline{6}$	660.5	4.4	6	688.9
$\underline{7}$	749.9	8.3	7	725.6
$\underline{8}$	789.3	8.0	8	895.3
$\underline{9}$	908.2	8.0	9	972.7
$\underline{10}$	1010.6	18.7	10	1063.9
$\underline{11}$	1067.0	7.5	11	1093.8
$\underline{12}$	1101.7	17.6	12	1119.1
$\underline{13}$	1117.5	10.9	13	1157.1
$\underline{14}$	1173.2	5.2	14	1191.1
$\underline{15}$	1201.4	8.4	15	1210.1
$\underline{16}$	1204.4	12.0	16	1222.9
$\underline{17}$	1308.6	13.0	17	1304.4
$\underline{18}$	1341.8	33.5	18	1343.3
$\underline{19}$	1382.9	9.5	19	1360.5
$\underline{20}$	1392.3	7.9	20	1379.0
$\underline{21}$	1408.8	26.0	21	1384.0
$\underline{22}$	1438.4	47.0	22	1444.7
$\underline{23}$	1490.6	20.1	23	1455.1
$\underline{24}$	1519.0	48.9	24	1477.7
$\underline{25}$	1546.8	43.4	25	1531.7
$\underline{26}$	1557.5	60.7	26	1571.7
			27	1588.4

We list in Table III the calculated frequencies of these modes and the values of $|\omega_\mu^0 - \omega_\mu^1|$. In the vibronic calculations, we fixed λ_μ to 2 for all configurations except the configurations $2^2\ \underline{4}$ and $2\ \underline{10}$. We also ignored configurations with $V' < 0.5$ cm^{-1}. A 234×234 vibronic matrix was thus obtained. In the calculations, we varied the energy separation between $S_1(0)$ and $S_2(0)$ and the λ_μ values of the configurations $2^2\ \underline{4}$ and $2\ \underline{10}$ until a good agreement of the calculated vibronic spectrum with the experimental spectrum was achieved. We then shifted the calculated vibronic spectrum to the experimentally determined position and corrected the energies of $S_1(0)$ and $S_2(0)$ accordingly.

The final calculated vibronic spectrum is shown in Fig. 4 along with the experimental spectrum. Major spectral features are numbered in the calculated spectrum. As shown in Fig. 4, the calculated spectrum reproduces the major spectral features in the 26 950–27 300-cm^{-1} spectral range very well. The energies, the first four leading vibronic configurations

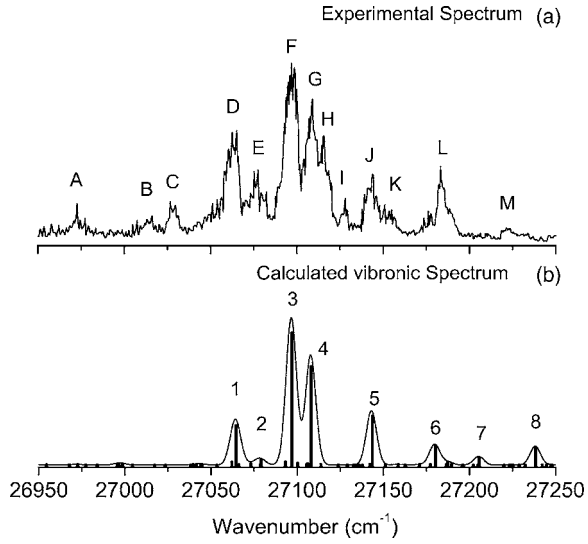

FIG. 4. Comparison of the (a) experimental and (b) calculated vibronic spectra of the $S_2 \leftarrow S_0$ and $S_2 \leftarrow S_0$ transitions of benzo[ghi]perylene. The calculated spectra are shown in stick spectrum and in convoluted spectrum with a Gaussian function of σ=7.0 cm^{-1}. The vibronic model employed in the calculations is discussed in the text.

and the values of $|a_2^n|^2$ of the major spectral features of the calculated spectrum are presented in Table IV. The determined separation between $S_1(0)$ and $S_2(0)$ is 1337 cm^{-1}, which matches with the experimental value of 1310 cm^{-1} very well. The final λ_μ values of the configurations $2^2\ \underline{4}$ and $2\ \underline{10}$ are both 4.0. The purpose of the variation of these two values is to adjust the relative intensities of features 4 and 6. All other features are found to be insensitive to the change of these two values. The determined energies of $S_1(0)$ and $S_2(0)$ are 25 795 and 27 132 cm^{-1}, respectively. These energies are listed in Table II as experimentally derived excitation energies.

IV. DISCUSSION

In this paper, we have reported the cavity ring-down spectrum of benzo[ghi]perylene in the 26 950–28 600-cm^{-1} spectral range for the first time. The spectral features are assigned to the vibronically coupled S_1 ($^1A_1$)$\leftarrow S_0$ ($^1A_1$) and S_2 ($^1B_1$)$\leftarrow S_0$ ($^1A_1$) electronic transitions. Due to the breakdown of the BO approximation and the resulting vibronic interaction, we found that the FC approximation fails to predict a satisfactory spectrum. With a simple vibronic model, we calculated the vibronic spectrum in the 26 950–27 300-cm^{-1} spectral range. The agreement of the calculated vibronic spectrum with the experimental spectrum is found to be satisfactory. Major spectral vibronic features (bands *D*, *E*, *F*, *G*, *J*, and *L*) can be assigned accordingly. We found that the TDA is superior to the RPA in calculating the excitation energies of the low-lying electronic states of neutral benzo[ghi]perylene. As shown in this work, the TDA predicts a reliable energy for the ^1L_a (S_2) state while it still overestimates the ^1L_b (S_1) state. However, in contrast with the RPA, the ordering of these two states is correctly retained in the TDA. It would be of great interest to check if this argument also applies to other neutral PAHs.

TABLE IV. Energies, the first four leading vibronic configurations and the values of $|a_2^n|^2$ of the calculated major spectral features in the 26 950–27 300-cm^{-1} spectral range.

Feature	Energy	$\lvert a_2^n\rvert^2$	Leading configurations
1	27 064.5	0.0917	$2^2\ \underline{4}+S_2(0)+1\ 4\ \underline{4}+2\ \underline{9}$
2	27 079.0	0.0123	$1\ \underline{10}+2\ 5\ \underline{2}+2^2\ \underline{4}+S_2(0)$
3	27 096.8	0.308	$\underline{17}+S_2(0)+\underline{18}+2^2\ \underline{4}$
4	27 108.0	0.230	$\underline{17}+S_2(0)+\underline{18}+1^2\ 2\ \underline{2}$
5	27 143.6	0.114	$\underline{18}+S_2(0)+2\ \underline{10}+3\ \underline{9}$
6	27 180.2	0.0431	$2\ \underline{10}+\underline{19}+S_2(0)+\underline{20}$
7	27 205.4	0.0183	$\underline{21}+S_2(0)+\underline{22}+2\ 3\ \underline{5}$
8	27 238.4	0.0395	$\underline{22}+S_2(0)+2\ \underline{11}+\underline{21}$

An important observation from this work is that the bandwidths of the observed spectral features are significantly broader than the expected rotational contour of benzo[ghi]perylene. Since the experiment was performed under very similar conditions as those used in the perylene experiment,[20] a similar rotational temperature (50–60 K) as derived from the perylene experiment is expected. The bandwidth of the spectral features of benzo[ghi]perylene, if solely determined by the rotational contour, is expected to be ca. 3 cm^{-1}. This value is significantly smaller than the measured values that range from 4.5 to 7.5 cm^{-1} (with corresponding lifetimes of 0.7–1.2 ps). This broadening can be attributed to the internal-conversion process via the strong vibronic interaction between the S_1 and S_2 states and the intersystem crossing to the nearby triplet states. As shown in Table II, several nearby triplet states, i.e., T_2 ($^3A_1$), T_3 ($^3A_1$), and T_6 ($^3A_1$), can couple to the S_2 state via the spin-orbit interaction. It would be of great interest to determine the relative contributions of these two processes to the spectral broadening. This cannot be achieved with CRDS and requires fluorescence excitation and emission experiments that can also provide invaluable information about the vibrational energies of both the lower and upper electronic manifolds. The fluorescence properties such as the fluorescence rate constant, fluorescent lifetimes, and quantum yields of benzo[ghi]perylene have been reported by Nijegorodov *et al.* in the solution and in the solid phase.[42] We defer further discussions of these properties and refer the interested readers to the original paper since the experiment was not done in the gas phase. It is our hope that this work will motivate further experimental and theoretical investigations of gas-phase benzo[ghi]perylene and larger PAHs.

ACKNOWLEDGMENTS

This research was performed while one of the authors (X.T.) held a National Research Council Research Associateship Award at NASA Ames Research Center. The authors want to thank Robert Walker for outstanding technical support. This research is supported by NASA's Space Mission Directorate (APRA program, RTOP 188-01-03-01).

[1] *The Diffuse Interstellar Bands*, edited by A. G. G. M. Tielens and T. P. Snow (Kluwer Academic, Dordrecht, 1995).
[2] G. P. van der Zwet and L. J. Allamandola, Astron. Astrophys. **146**, 76 (1985).
[3] A. Léger and L. B. d'Hendecourt, Astron. Astrophys. **146**, 81 (1985).
[4] F. Salama, E. L. O. Bakes, L. J. Allamandola, and A. G. G. M. Tielens, Astrophys. J. **458**, 621 (1996).
[5] G. H. Herbig, Annu. Rev. Astron. Astrophys. **33**, 19 (1995).
[6] S. O. Tuairisg, J. Cami, B. H. Foing, P. Sonnentrucker, and P. Ehrenfreund, Astron. Astrophys., Suppl. Ser. **142**, 225 (2000).
[7] F. Salama and L. J. Allamandola, J. Chem. Phys. **94**, 6964 (1991).
[8] F. Salama, C. Joblin, and L. J. Allamandola, J. Chem. Phys. **101**, 10252 (1994).
[9] F. Salama, *Low Temperature Molecular Spectroscopy* (Kluwer, Dordrecht, 1996), p. 169.
[10] G. Berden, R. Peeters, and G. Meijer, Int. Rev. Phys. Chem. **19**, 565 (2000).
[11] J. M. Herbelin, J. A. Mckay, M. A. Kwok, R. H. Ueunten, D. S. Urevig, D. J. Spencer, and D. J. Benard, Appl. Opt. **19**, 144 (1980).
[12] D. Z. Anderson, J. C. Frisch, and C. S. Masser, Appl. Opt. **23**, 1238 (1984).
[13] A. O'Keefe and D. A. G. Deacon, Rev. Sci. Instrum. **59**, 2544 (1988).
[14] D. Romanini, L. Biennier, F. Salama, A. Kachanov, L. J. Allamandola, and F. Stoeckel, Chem. Phys. Lett. **303**, 165 (1999).
[15] L. Biennier, F. Salama, L. J. Allamandola, and J. J. Scherer, J. Chem. Phys. **118**, 7863 (2003).
[16] L. Biennier, F. Salama, M. Gupta, and A. O'Keefe, Chem. Phys. Lett. **387**, 287 (2004).
[17] O. Sukhorukov, A. Staicu, E. Diegel, G. Rouillé, T. Henning, and F. Huisken, Chem. Phys. Lett. **386**, 259 (2004).
[18] G. Rouillé, S. Krasnokutski, F. Huisken, T. Henning, O. Sukhorukov, and A. Staicu, J. Chem. Phys. **120**, 6028 (2004).
[19] A. Staicu, O. Sukhorukov, G. Rouillé, T. Henning, and F. Huisken, Mol. Phys. **102**, 1777 (2004).
[20] X. Tan and F. Salama, J. Chem. Phys. **122**, 084318 (2005).
[21] K. Liu, R. S. Fellers, M. R. Viant, R. P. Mclaughlin, M. Brown, and R. Saykally, Rev. Sci. Instrum. **67**, 410 (1996).
[22] X. Chillier, P. Boulet, H. Chermette, F. Salama, and J. Weber, J. Chem. Phys. **115**, 1769 (2001).
[23] V. Oja and E. M. Suuberg, J. Chem. Eng. Data **43**, 486 (1998).
[24] P. Hohenberg and W. Kohn, Phys. Rev. B **136**, 864 (1964).
[25] W. Kohn and L. J. Sham, Phys. Rev. A **140**, 1133 (1965).
[26] R. G. Parr and W. Yang, *Density-Functional Theory of Atoms and Molecules* (Oxford University Press, Oxford, 1989).
[27] E. K. U. Gross, J. F. Dobson, and M. Petersilka, Top. Curr. Chem. **181**, 81 (1996).
[28] R. Bauernschmitt and R. Ahlrichs, Chem. Phys. Lett. **256**, 454 (1996).
[29] A. D. Becke, J. Chem. Phys. **98**, 5648 (1993).
[30] C. Lee, W. Yang, and R. G. Parr, Phys. Rev. B **37**, 785 (1988).
[31] B. Miehlich, A. Savin, H. Stoll, and H. Preuss, Chem. Phys. Lett. **157**, 200 (1989).
[32] A. D. Becke, Phys. Rev. A **36**, 3098 (1988).
[33] J. P. Perdew, Phys. Rev. B **33**, 8822 (1986).
[34] K. Eichkorn, O. Treutler, H. Öhm, M. Häser, and R. Ahlrichs, Chem. Phys. Lett. **242**, 652 (1995).
[35] K. Eichkorn, F. Weigend, O. Treutler, and R. Ahlrichs, Theor. Chem. Acc. **97**, 119 (1997).
[36] A. Schäfer, H. Horn, and R. Ahlrichs, J. Chem. Phys. **97**, 2571 (1992).
[37] S. Hirata and M. Head-Gordon, Chem. Phys. Lett. **314**, 291 (1999).
[38] T. D. Bouman and A. E. Hansen, Int. J. Quantum Chem., Quantum Chem. Symp. **23**, 381 (1989).
[39] A. E. Hansen, B. Voigt, and S. Rettrup, Int. J. Quantum Chem. **23**, 595 (1983).
[40] R. Ahlrichs, M. Bär, M. Häser, H. Horn, and C. Kölmel, Chem. Phys. Lett. **162**, 165 (1989).
[41] J. R. Platt, J. Chem. Phys. **17**, 484 (1949).
[42] N. Nijegorodov, R. Mabbs, and W. S. Downey, Spectrochim. Acta, Part A **57**, 2673 (2001).
[43] M. Parac and S. Grimme, Chem. Phys. **292**, 11 (2003).
[44] R. Borrelli and A. Peluso, J. Chem. Phys. **119**, 8437 (2003).
[45] N. Ohta, H. Baba, and G. Marconi, Chem. Phys. Lett. **133**, 222 (1987).
[46] E. A. Mangle and M. R. Topp, J. Phys. Chem. **90**, 802 (1986).
[47] J. Wessel and D. S. McClure, Mol. Cryst. Liq. Cryst. **58**, 121 (1980).
[48] A. R. Lacey, E. F. McCoy, and I. G. Ross, Chem. Phys. Lett. **21**, 233 (1973).
[49] G. Fischer, Chem. Phys. **4**, 62 (1974).
[50] R. M. Hochstrasser, Acc. Chem. Res. **1**, 266 (1968).
[51] K. Ohno, Chem. Phys. Lett. **64**, 560 (1979).
[52] K. Ohno and R. Takahashi, Chem. Phys. Lett. **356**, 409 (2002).